SUPPRESSION OF BIODYNAMIC INTERFERENCE IN HEAD-TRACKED TELEOPERATION

S. Lifshitz, S. J. Merhav and A. J. Grunwald
Department of Aerospace Engineering, Technion, Haifa, Israel

G. E. Tucker
NASA Ames Research Center, Moffett Field, CA, USA

M. B. Tischler
U.S. Army Aeroflightdynamics Directorate, Moffett Field, CA, USA

Abstract

The utility of helmet-tracked sights to provide pointing commands for teleoperation of cameras, lasers, or antennas in aircraft is degraded by the presence of uncommanded, involuntary head motion, referred to as biodynamic interference. This interference limits the achievable precision required in pointing tasks. The noise contributions due to biodynamic interference consist of an additive component which is correlated with aircraft vibration and an uncorrelated, nonadditive component, referred to as remnant. In this paper, an experimental simulation study is described which investigated the improvements achievable in pointing and tracking precision using dynamic display shifting in the helmet-mounted display. The experiment was conducted in a six-degree-of-freedom motion base simulator with an emulated helmet-mounted sight. Highly experienced pilot subjects performed precision head-pointing tasks while manually flying a visual flight-path tracking task. Four schemes using adaptive and low-pass filtering of the head motion were evaluated to determine their effects on task performance and pilot workload in the presence of whole-body vibration characteristic of helicopter flight. The results indicate that, for tracking tasks involving continuously moving targets, improvements of up to 70% can be achieved in percent on-target dwelling time and of up to 35% in rms tracking error, with the adaptive plus low-pass filter configuration. The results with the same filter configuration for the task of capturing randomly-positioned, stationary targets show an increase of up to 340% in the number of targets captured and an improvement of up to 24% in the average capture time. The adaptive plus low-pass filter combination was considered to exhibit the best overall display dynamics by each of the subjects.

List of Symbols

a, a'	acceleration
e	adaptive algorithm convergence error
g	gravity acceleration
N_{na}	nonadditive, nonvoluntary head motion
$\hat{N}_{na}$	estimated nonadditive, nonvoluntary head motion
U_b	nonvoluntary head motion
$\hat{U}_b$	estimated additive, nonvoluntary head motion
$\tilde{U}_b$	additive, nonvoluntary head motion estimation error
U_c	voluntary head motion
U_f	estimated voluntary head motion
U_t	total head motion
W	adaptive filter weights vector
X_r, Y_r	reticle position
X_t, Y_t	target position
Y_b	biodynamic transfer function
$\alpha, \alpha_r, \alpha_s$	angles
μ	adaptive filter gain

Introduction

Air combat and attack missions in modern warfare subject the pilot to heavy workload. A major technological goal is to reduce this workload by using a helmet-mounted display (HMD) and by slaving teleoperated devices to head angular motion. However, aircraft vibration and buffeting cause unintentional head motion, referred to as "biodynamic interference" (Refs 1,2), which, in turn, causes vision blurring in HMDs (Refs 3,4) and degradation of the needed tracking and pointing accuracy (Refs 5,6).

This paper discusses a method for reducing the effects of vibrations on the precision of pilot pointing and tracking. Research results presented herein are an outcome of cooperation under the U.S./Israel Memorandum of Understanding (MOU) on Helicopter Flight Control and Display

Technology. The overall approach taken is to estimate, in real time, the nonvoluntary components of head motion and to use these signals to stabilize the symbols in the image plane of the display. This image stabilization reduces the blurring perceived by the pilot involved in viewing tasks (Ref 7) and allows increased pointing precision. However, there is an important distinction between the stabilization required for viewing tasks and that required for tracking tasks. In the viewing task, the dominant interference is additive and can be handled by noise cancellation methods. In the tracking task, however, the remnant noise increases with the intensity of the vibration and can become dominant. The remnant noise is not additive and, therefore, cannot be directly reduced by the noise cancellation method (Ref 7). As a result, additional filters are needed to reduce the effects of nonadditive biodynamic interference.

The helmet-mounted sight (HMS) enables head teleoperation of devices for pointing or tracking (Ref 8). The helmet is equipped with a sensor which measures head orientation and position with respect to a cockpit-based reference system. The sight reticle, focused to near infinity, is projected onto the semi-transparent helmet visor allowing the acquisition and tracking of targets. The precision with which this task can be accomplished is affected by the uncommanded translational and angular vibration of the head. The resulting tracking error has been found to increase with increased pilot workload (Ref 9). Wells and Griffin (Ref 5), who have studied the biodynamic interference phenomenon both in the laboratory and in flight, divided the factors which influence tracking precision into three categories, namely:

1. Minor effects: Apparent target size, the shape of the reticle, right or left eye, seat type, helmet weight, elevation of line of sight, nature of secondary task.

2. Significant effects: Size of the reticle, azimuth of line of sight.

3. Major effects: Head vibration, target motion.

Griffin and Wells (Ref 6) investigated, under laboratory conditions, by means of a helmet sight, the effects of head vibration and target motion on tracking error. The most pronounced increase in tracking error was in the region from 3-5 Hz, where the biodynamic feedthrough from seat to head is the largest.

The effects of vibration filtering on tracking precision was investigated by Lifshitz and Merhav in a previous simulation experiment (Ref 10). The method presented for improving aiming accuracy is based on head motion measurement and on the shifting of the reticle in the HMD in such a way as to inhibit much of the apparent motion of the reticle. The reticle shift algorithm also provides stabilization signals to prevent the teleoperated device from

following the nonvoluntary motion of the head. The subjects were instructed to track a stationary or randomly maneuvering target (in elevation only) using an emulated HMS incorporating dynamic display shifts by means of adaptive and low-pass filtering in elevation only. The subjects were vibrated vertically in a six-degree-of-freedom motion base simulator with acceleration amplitudes of 0.3-0.7 m/sec^2 rms using sinusoidal and random motions. The subjects' only task was target tracking. The results show that, with an adaptive filter, an improvement of 8-14% in on-target reticle dwelling time and tracking rms error was achieved. Using only low-pass filtering, tracking performance was improved by 34-50%. With the combined adaptive and low-pass filtering configuration, improvements of 30-60% were found, depending on vibration level and type, and the maneuverability of the target.

The present paper is an extension of the above experiments. Here, multi-axis head-pointing tasks in the presence of a secondary vehicle control task were presented to four pilot subjects. All of the subject pilots are active helicopter pilots with considerable experience in military rotorcraft missions. The results show that improvements of up to 70% can be achieved in percent on-target dwelling time and of up to 35% in the rms tracking error, with the combined adaptive plus low-pass filter configuration. The results with the same filter configuration for the task of capturing randomly-positioned stationary targets show an improvement of up to 340% in the number of targets captured and a reduction of up to 24% in the average time required to achieve capture. The adaptive plus low-pass filter combination was considered to exhibit the best overall display dynamics by each of the subjects.

Principle of Display Stabilization

The method for stabilizing a true HMD is illustrated in Fig 1. The target, A/C, is viewed through the semi-transparent visor from which the display is reflected to the pilot's eye. The hexagon, S, represents a display element projected to infinity. The acceleration, a, excites the biodynamic interferences in the human operator which is described by the biodynamic model, Y_b. The biodynamic interference manifests itself as a vertical head vibration accompanied by an angular head vibration of amplitude, α, which causes S to shift with respect to A/C. The image of A/C on the retina remains fixed, and therefore sharp, under vibrational conditions which are within the range of the vestibulo-ocular stabilizing mechanism. However, the image of S, fixed to the display, moves across the retina causing S to appear blurred.

The head motion sensor, P, provides head position and orientation signals with respect to the cockpit. These signals consist of the voluntary (commanded) head motion, U_c, and the nonvoluntary head motion (biodynamic interference), U_b, which, in the case described here, is the head

$$U_t = U_c + U_b$$

ACCELERO-METER a'

TO TELEOPERATED DEVICE

DISPLAY GENERATOR $\hat{U}_b$ ADAPTIVE ALGORITHM U_f LPF

$\hat{N}_{na}$

CANOPY P HMD HEAD MOTION SHIFTED DISPLAY s' A/C

$-\alpha_s$ VESTIBULARLY STABILIZED LOS STABILIZED DISPLAY, S
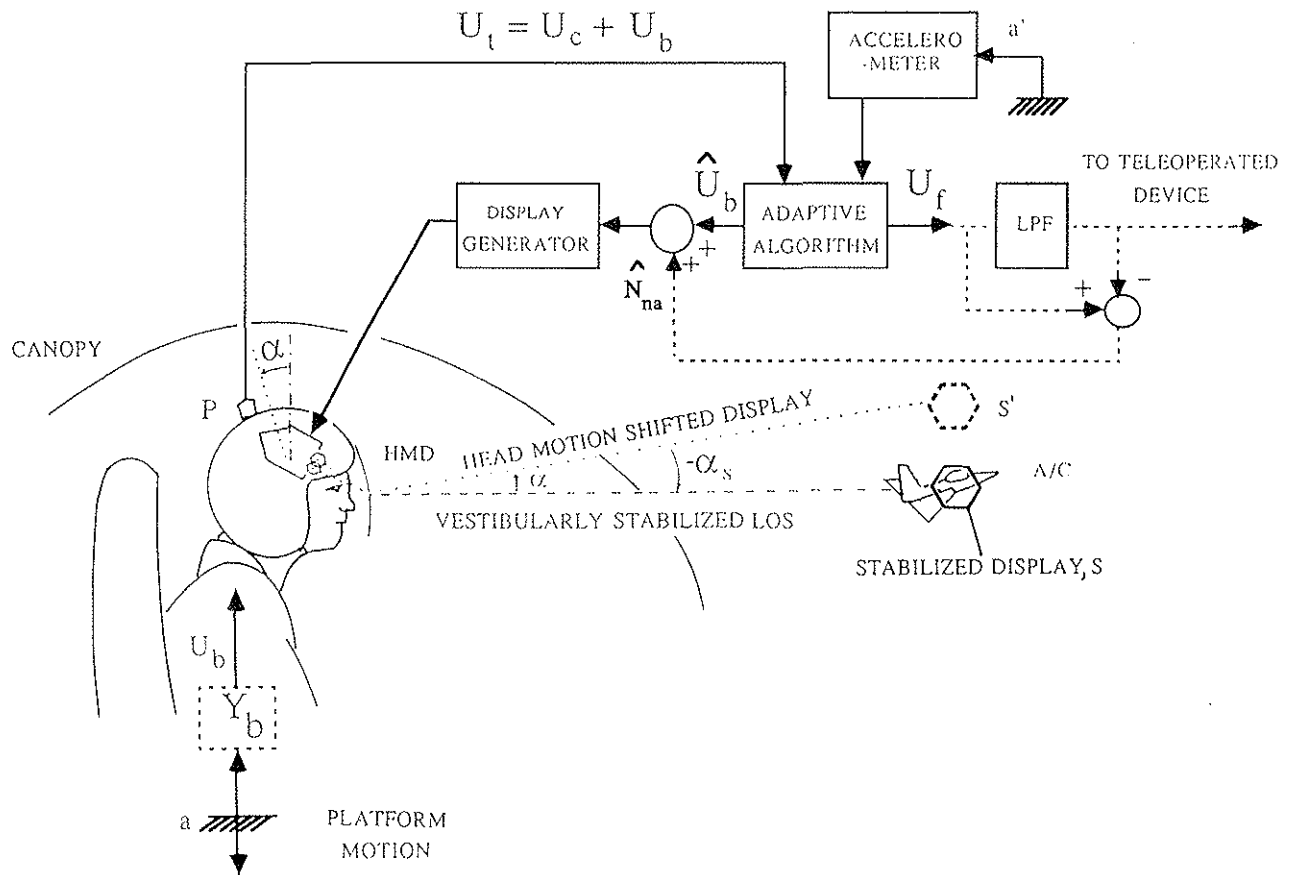
U_b Y_b a PLATFORM MOTION

Fig 1. Principle of display image stabilization.

pitching motion. The total head motion is defined as $U_t = U_c + U_b$. The adaptive algorithm provides estimated values: $\hat{U}_b$ of U_b and U_f of U_c which is derived from $U_f = U_t - \hat{U}_b$. In order to stabilize display elements against the additive vibration component in a purely viewing task, $\hat{U}_b$ is fed into the display generator in opposite phase to the apparent shift of S, so that S appears to be stationary. This method of stabilization is shown in solid lines in Fig 1.

In order to facilitate smooth head teleoperation of a device, additional filtering of the reticle drive signal must be provided to compensate for the nonadditive, nonvoluntary (remnant) head motion components, Nna. Not being directly correlated with the cockpit motion, remnant cannot be suppressed by the adaptive algorithm alone. Therefore, these components give rise to additional relative shifts between the eye and the display and impair target acquisition and tracking. The commanded head motion, U_c, is by nature of much lower frequency than the uncommanded signal, U_b. Therefore, U_f, which is an estimate of U_c, is low-pass filtered to attenuate N_{na}. The resulting low-pass filtered U_f is then used in two ways as illustrated by the dashed lines in Fig 1.

First, the filtered U_f signal is subtracted from the unfiltered U_f signal (equivalent to high-pass filtering U_f) to yield the estimated remnant signal $\hat{N}_{na}$. This estimated remnant is added to the estimated vibration-correlated interference $\hat{U}_b$ to obtain an estimate of the total biodynamic interference signal U_b. This final estimate of nonvoluntary head motion is fed into the display generator in opposite phase with the measured head motion. The result is a non-blurred sight stabilized against U_b and N_{na}. Finally, the low-pass filtered U_f signal is fed to the head-slaved teleoperated device. The result is good correspondence between the slaved device and the voluntary head motion. In addition, the slaved device is not required to cope with high frequencies which may be outside its servo bandwidth.

The stabilization scheme in Fig 1 was discussed with respect to the elevation axis only. For a fully operational system, the filter scheme would be implemented for the azimuth axis as well.

Experimental Investigation

The experimental program had two main goals:

1.   To determine the effects of vibration on head-pointing accuracy in the presence of a secondary piloting task.

2.   To quantify the contribution of the various filtering schemes to head-pointing precision.

Experimental Set-up

An overall view of the experimental set-up is shown in Fig 2. The set-up consisted of the following elements:

- Six-degree-of-freedom motion simulator

- Six-degree-of-freedom head motion (Polhemus) sensor

- Cabin floor-mounted accelerometer

- Lightweight helmet equipped with the head motion sensor and intercom

- Data acquisition and communication system

- DEC Vax 750

- Motorola VME System 1131

- SiliconGraphics Iris-4D 50 GT graphics station

- Image Technology, Inc., Series 100 Image Processor (FG-100)
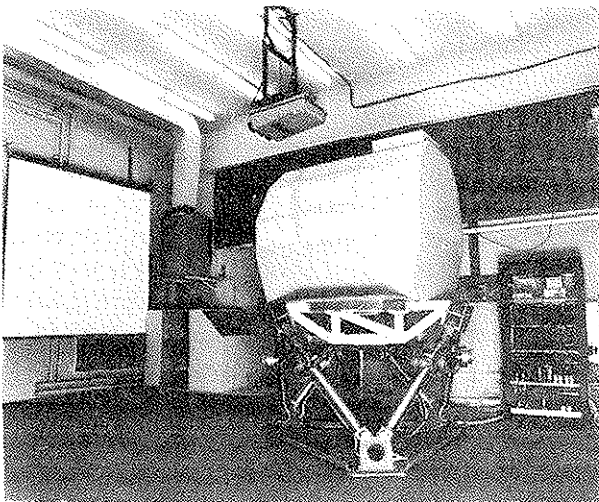
- Barco overhead TV projector.

Fig 2. Experimental set-up.

A detailed description of its principal subsystems is provided below.

Six-degree-of-freedom motion based simulator. The simulator was designed and developed at the Technion's Aerospace Flight Control laboratory. It has an electrome-chanical hexapod drive system (Steward platform) using high-torque samarium-cobalt D. C. motors. It is digitally-controlled and accepts commands from inside the cabin in

addition to external computer commands. Its bandwidth is approximately 15 Hz and its motion limits are approximately 0.5 meters in translation and 30 deg in rotation. The maximum acceleration capability is 1g. The cabin construction is wood and plastic to avoid interference with the electromagnetic head motion sensor.

Head motion sensor. The head motion sensor is a Polhemus "3space Tracker." It consists of (1) the system electronics unit; (2) the source, or transmitter, which is mounted in the canopy above the head; and (3) the sensor, which is mounted on the helmet. The maximum sampling rate of the Polhemus is 60 Hz, but communication system limitations reduce the actual sampling rate to 37 Hz. The static precision in translation is 2.5 mm (rms) and the angular precision is 0.5 deg (rms). The resolution in translation is 0.75 mm and 0.1 deg in rotation. Position measurements are transmitted to the computer serially via a RS232 communication board.

Helmet-mounted sight emulation. In the experiments described here, an actual helmet sight was not yet available. Therefore, the simulations were performed by emulating the helmet sight as illustrated in Fig 3. The square, r, represented a collimated reticle in an actual display, subtended an arc 0.65 deg high and 0.65 deg wide. The target, t, represented by a cross, subtended an arc 0.15 deg high and 0.21 deg wide. Both symbols were projected on a screen with a display area 14 deg high and 22 deg wide placed 5 meters in front of the subject. The shifting of the square on the screen, in response to angular head motion, U_t, was therefore an emulation of a nonstabilized HMD sight, and was implemented by means of the Polhemus signals. In order to stabilize the reticle in an actual HMD, the square must be shifted in accordance with $\hat{U}_b$ and $\hat{N}_{na}$ (Fig 1). However, when *emulating* the sight dynamics, the command for image stabilization is $U_t - \hat{U}_b = U_f$ (Fig 3). Further low-pass filtering of U_f prior to the projector, in the emulation, is equivalent to adding a high-pass filtered (HPF) U_f to $\hat{U}_b$ in the actual display to attenuate N_{na}.

It must be emphasized that in the experiments discussed herein, the adaptive filter was implemented in the elevation axis only, due to current computational limitations.

System Integration. The system block diagram is presented in Fig 4.

The simulator vibration motion was computed off-line in the Motorola computer and fed to the motor amplifiers at 148 Hz. The vertical cabin acceleration, a, provided by the accelerometer was smoothed by a 15 Hz low-pass filter and sampled by an A/D converter to provide a' which was fed to the Motorola computer. Depending on the filter combination, the inputs into the reticle position shifting algorithm were
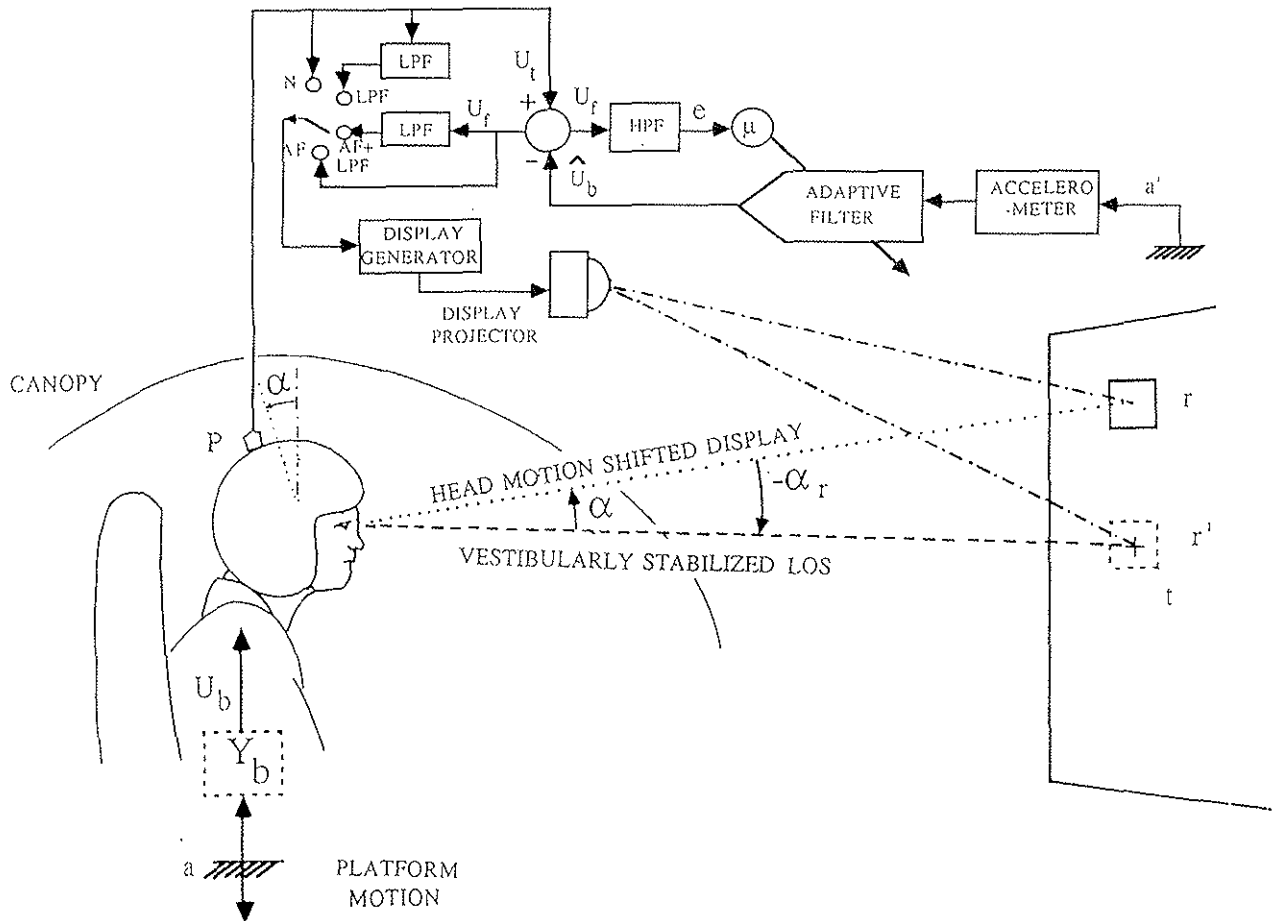
CANOPY

N

LPF
LPF
AF+ LPF
AF

U_t

U_f
+
U_f
HPF
e
μ

ADAPTIVE FILTER

ACCELERO-METER

a'

$\hat{U}_b$

DISPLAY GENERATOR

DISPLAY PROJECTOR

r

r'

t

α

P

HEAD MOTION SHIFTED DISPLAY

α

$-\alpha_r$

VESTIBULARLY STABILIZED LOS

U_b

Y_b

a

PLATFORM MOTION

Fig 3. Helmet-mounted sight emulation.

BARCO PROJECTOR

SILICON GRAPHICS IRIS 4D

SIMULATOR MASTER CONTROLLER

VAX 750

DISPLAY GENERATOR

MOTOR COMMANDS PROGRAM

SIMULATOR BOARD

D/A

SIX MOTORS

ΔX_t ΔY_t ΔY_r ΔX_r

$LPF\{U_f\}$
$LPF\{U_t\}$
U_f
U_t

ADAPTIVE ALGORITHM

a'

A/D

LPF

ACCELERO-METER

RETICLE POSITION SHIFTS ALGORITHM

U_t

TARGET DYNAMICS

X_r Y_r U_t U_f $\hat{U}_b$ e a'

Y_t

X_t

DATA FILE

COMMUNICATIONS BOARD

U_t

POLHEMUS

X_r Y_r X_t Y_t

PERFORMANCE PROCESSING

LEGEND:
OFF LINE
ON LINE

SIMULATOR CABIN

VIAE SYSTEM 1131
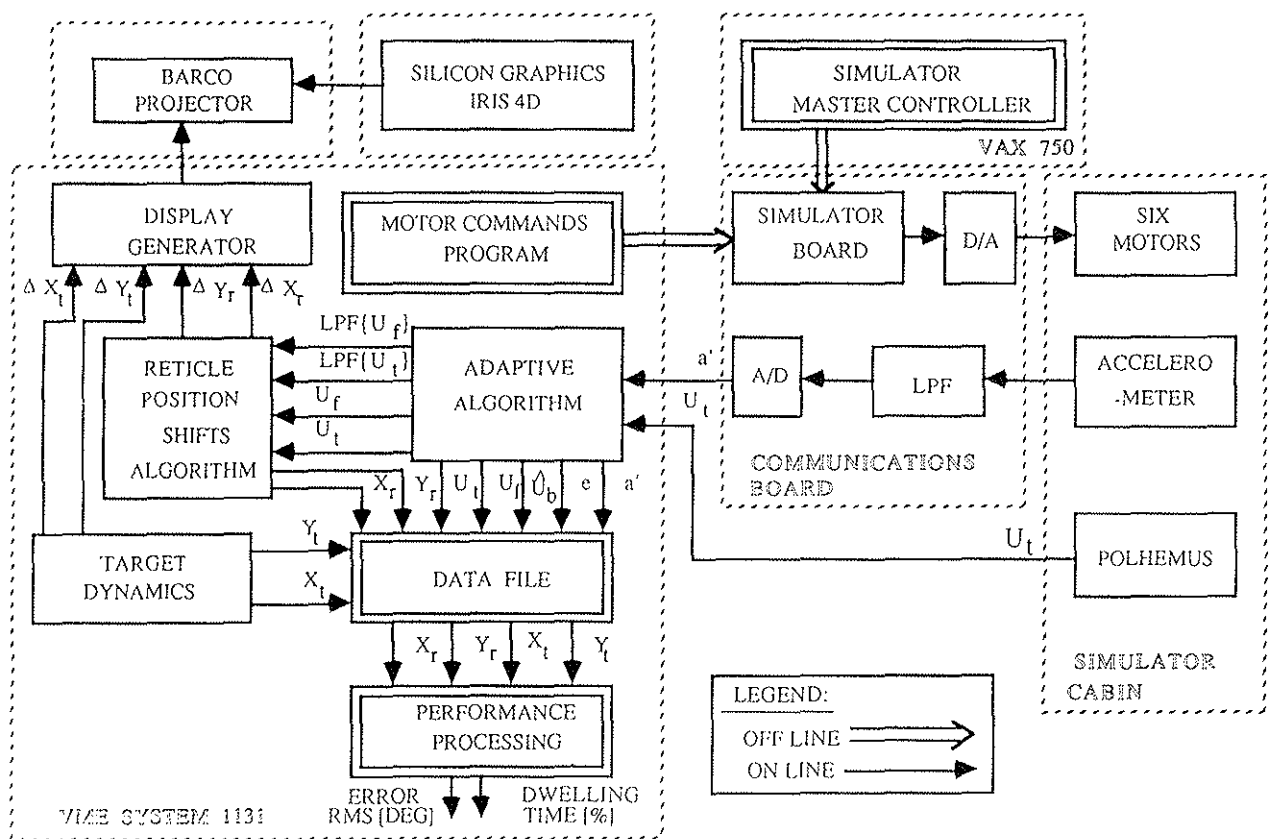
ERROR RMS [DEG]

DWELLING TIME [%]

Fig 4. System block diagram.

In Azimuth:

- U_t
- Low-pass filtered (LPF) U_t

In Elevation:

- U_t
- Low-pass filtered U_t
- U_f
- Low-pass filtered U_f

Both the outputs of the reticle position shifting algorithm and the target dynamics were fed into the display generator which drove the overhead TV projector. For each run, the following data were recorded: U_t, U_b, U_f, a', and the adaptive algorithm convergence error, e. Target position, X_t, Y_t, and reticle position, X_r, Y_r, were processed after each run in order to enable immediate assessment of the performance of the subject.

Simulation Tasks Description

Two primary precision head-pointing experiments were performed, each with the same secondary flight control task:

Experiment 1: Tracking a continuously maneuvering target.

Task description: Each subject trial started with 15 seconds of exposure to the vertical vibration while manually flying the secondary tracking task described below. This initial segment allowed the adaptive filter to converge and the pilot to comfortably settle his body postion while getting used to the sidearm controller characteristics. Following this initial 15-second period, the reticle appeared centered over the target, in the center of the display field. During the next 60 seconds the subject was instructed to keep the reticle tightly centered over the randomly moving target while continuing to "fly" the secondary tracking task.

Simulator motion: Vertical, sum of sines at frequencies of 5 Hz and 10 Hz, plus a random component derived from zero mean gaussian white noise filtered by a second-order LPF with damping ratio of 0.5 and cut-off frequency of 0.5 Hz, representing low-frequency turbulence. Acceleration amplitude was 0.073 g rms, with peak values of 0.5 g.

This vibration spectrum was chosen quantitatively and qualitatively to simulate the periodic frequency content of an AH-1S Cobra's two-bladed, teetering rotor system at cruise airspeed in low frequency, moderate turbulence. The intensity levels and inclusion of a turbulence model were selected to demonstrate differences between filter combinations under challenging but operationally realistic conditions.

Target characteristics: Two unique, randomly-generated target motions with amplitudes ranging from 1.6-1.9 deg rms in azimuth and 1.3-1.5 deg rms in elevation were selectively presented to the subjects. Target rms velocities were 0.20-0.27 deg/sec in azimuth and 0.20-0.22 deg/sec in elevation.

Number of subjects: 3.

Experiment 2: Discrete stationary target acquisition.

Task description: Each subject trial started with 15 seconds of exposure to the vertical vibration while manually flying the secondary tracking task. Following the initial 15 seconds of secondary task performance, the reticle appeared in the middle of the display area simultaneously with the first target. Individual targets sequentially appeared at random positions in the display field for a maximum of 10 seconds. If, during this period, the subject was able to position the reticle so that it completely enclosed the target for 2.7 seconds, a "capture" would be recorded, the reticle would change from fluorescent green to fluorescent red, and the target would disappear. After an additional 2 seconds, the reticle color would reset to green followed by the appearance of a new target. If the subject was not successful in meeting the 2.7-second criteria within the allowed 10 seconds, a "miss" would be recorded, and the target would disappear for 5 seconds followed by the appearance of a new target. Subjects were instructed to acquire each target in minimum time in order to maximize the total number of targets presented in the fixed trial time.

Target characteristics: Four unique, randomly-generated target sets were available for presentation to the subject.

Simulator motion: Vertical, sum of sines at frequencies of 5 Hz and 10 Hz. Acceleration 0.043 g rms, 0.16 g peak to peak.

Number of Subjects: 4.

Secondary control task: The secondary control task required the pilot to manually control the apparent flight path of the simulated helicopter along a curved spatial trajectory represented by a pictoral "tunnel-in-the-sky" (Fig 5), (Refs 11,12,13). The tunnel image was generated on-line by the IRIS 4D/50 GT graphics work station and relayed to the Barco projector where it was mixed with the emulated target and reticle images. Although projected as part of a composite image, the tunnel was inertially fixed on the projection screen and unaffected by cabin motion. The tunnel had a square cross section 300 ft wide and was 33,200 ft long, consisting of 4 straight and 3 curved sections with constant rate left- and right-banked turns. The vertical profile consisted of one level and two descending sections with slopes of 6% and 8%.
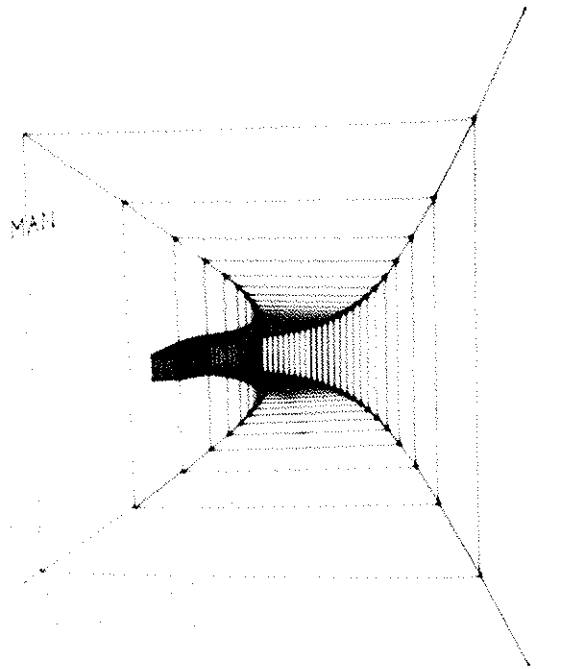
Fig 5. Pictorial "tunnel-in-the-sky."

The subjects were instructed to keep the vehicle as close as possible to the center of the tunnel both laterally and vertically using a side-arm force controller installed with an arm rest on the right side of the pilot's seat. A beeping audio tone was fed to the subject's earphones if the tunnel boundary was exceeded and doubled in frequency if the exceedence was greater than one tunnel width. The longitudinal control model represented a vehicle with an ideal airspeed hold (constant speed of 120 kt) and ideal zero angle of attack. The longitudinal controller commanded pitch attitude with dynamics approximated by a first-order lag with a break frequency of 0.5 rad/sec. In the roll axis the model was a rate command system with ideal turn coordination. Dynamics were approximated by a well damped second-order system with a bandwidth of 5 rad/sec. The predictability of the required flight path, as viewed by the subject, was reduced by randomly presenting a horizontally-mirrored image of the original tunnel path.

Configurations Evaluated

In each of the two experiments, the following filter/vibration combinations were tested:

1. Stationary cabin (Static).

2. Vibrating cabin, unstabilized sight (No Filtering).

3. Vibrating cabin, sight stabilized only by an adaptive filter (AF) in elevation only.

4. Vibrating cabin, sight stabilized only by low-pass filtering (LPF) in elevation and azimuth.

5. Vibrating cabin, stabilized sight by adaptive and LPF (AF +LPF) in elevation and LPF only in azimuth.

The Subjects and Their Training

Four subjects participated in the pointing and tracking experiments. All of them are active helicopter pilots. Before starting the actual tests, the subjects underwent an initial training period in the simulator of approximately six hours each, in the course of which approximately 15 runs for each configuration were executed. After each subject reached a stable level of performance, data acquisition commenced. On the average, 20 runs were executed per hour.

The Adaptive and Low-Pass Filters

The AF is based on the well known least-mean-square (LMS) algorithm widely used in adaptive noise cancellation applications. It is an extension of the classical LMS described in Widrow and McCool (Ref 14). Its main advantages are small computational load, global stability, and robustness. The extended LMS presented in this paper has the additional advantages of rapid adaptation to variations in model parameters and the precise estimation of the relatively small disturbance, U_b, in the presence of large voluntary head motion, U_c. This issue is addressed in Merhav (Ref 15). Other algorithms such as root-least-square and Lattice filters, Haykin (Ref 16), Honig and Messerschmitt (Ref 14) were considered because of their

superior convergence in terms of the number of iterations. However, in view of their larger computational complexity, longer iteration times, and lower robustness where rapid variations in model parameters are involved, they were not adopted in the present study. In view of these considerations and the successful implementation of the basic LMS in suppressing biodynamic disturbances in manual control (Refs 17,18) the extended LMS was used in the work described here.

The break-point of the high-pass filter for U_t was set to 15 rad/sec since the dominant frequency of the nonvoluntary head motion was in the region of 4-5 Hz. On the average, the adaptive filter, as implemented in these experiments, converges in 2.5-3 seconds. The adaptive filter algorithm also incorporates a cut-off mechanism as explained in Ref 7. The cut-off frequency of the LPF for N_{na} was set to 2 rad/sec. This choice was a good compromise between the need to attenuate these noise components and to avoid excessive phase lag in the motion of the reticle. Excessive lag in the reticle for large head displacements was satisfactorily reduced by disconnecting the LPF when angular head rates exceeded 30 deg/sec. The LPF was reconnected exponentially when head angular rate decreased to less than 30 deg/sec.

Data Processing

Since $\hat{U}_b$ and U_f were estimated in the elevation axis only, data were processed accordingly and divided into two parts:

1. Evaluation of the performance of the AF: Analysis of the estimated signals $\hat{U}_b$ and U_f, the vector of weights, $\underline{W}$, and the convergence of adaptation error, e.

2. Evaluation of the performance of the human operator in head pointing and tracking experiments:

For Experiment 1:

a. The dwelling time of the reticle on the target: The percentage of time during a run within which the distance between the respective centers of the target and the reticle was smaller than half the height and width of the reticle.

b. The rms tracking error: The rms values of the distance between reticle and target centers were determined in elevation and azimuth.

For Experiment 2:

a. The total number of targets presented.

b. The percentage of targets "captured."

c. The average time per target "capture."

The performance of each subject was evaluated for each of the filter configurations in each of the two experiments. Ten data runs were taken per filter configuration per subject. Results were determined for each subject and were averaged across all subjects for each filter configuration in each of the two experiments.

Experimental Results

Experiment 1 - Target Tracking Task

On-target dwell time and radial tracking error are presented in Table 1. With no vibration, the reticle was "on-target," on the average, for more than 82% of the time and the rms pointing error was 0.192 deg. The periodic and turbulence-induced vibration caused a decrease in dwelling time to 37% and an increase in the pointing error to 0.437 degree rms, without filtering. With the AF, the percentage dwelling time increased by 11% with a decrease in tracking error of 9% relative to No Filtering. With the AF+LPF configuration, the percent dwelling time increased by 73% with a decrease in tracking error of 35% relative to No Filtering. With the LPF alone, the percent dwelling time increased 64% and the tracking error decreased 28%.

The No Filter configuration allowed the subject the greatest degree of direct control over the reticle (minimum

Table 1. Average Results of Target Tracking Experiment 1.

Configuration	Dwelling time (%)	Dwelling time improvement relative to no filtering (%)	Radial tracking error (deg)	Radial tracking error improvement relative to no filtering (%)
Stationary	82.8		0.192	
No filters	37.7		0.437	
AF	41.8	10.9	0.396	9.4
LPF	61.8	63.9	0.313	28.4
AF + LPF	65.1	72.7	0.284	35.0

lag), but passed all of the additive and non-additive vibration to the helmet sight. The result was a severe degradation of tracking performance.

The relatively small improvement in performance with the adaptive filter alone is explained by reference to Fig 6. Figure 6(a) shows an example of the total measured head motion while aiming at a stationary target and with a vibrating cabin. Most of the additive head motion is removed from the signal by the AF, as seen in Fig 6(b) from the lack of 5 Hz and 10 Hz additive vibration feedthrough. However, very little of the remaining remnant is suppressed since it is not correlated with cabin vibration and therefore cannot be suppressed by the AF. The non-correlated remnant head motion, accentuated by the random turbulence, severely disrupts the AF's convergence process, which on the average lasts 2.5-3 seconds. The filter-induced excitation of the reticle in elevation could not be eliminated by the pilot and occasionally caused a workload-related degradation in azimuth tracking performance as well. The most successful, but extremely limiting, pilot technique was to minimize unnecessary voluntary head motion and then to move the head only very slowly.

Only small differences were found between the respective performance with the LPF alone and the AF+LPF configurations. The primary reason is that the LPF, which was designed to suppress the non-additive biodynamic interference, N_{na}, attenuates most of the remnant noise, as seen in Fig 6(c), in addition to much of the additive interference. The addition of the AF to the LPF resulted in better suppression of the additive biodynamic component. Considering the narrow reticle positioning constraints of the tracking task (0.3 deg), the slight reduction in amplitude of the reticle motion when the AF and LPF were combined compared to the LPF-only case very likely accounted for the slightly higher scores achieved.

Subjects in this simulation indicated that, as they became more experienced, they learned how to achieve the optimum balance between general muscle relaxation and directed attention to the task, which significantly increased their overall performance.

Experiment 2 - Target Acquisition Task

From Table 2, one can see that, on average, both the total number of targets displayed and the percentage of targets
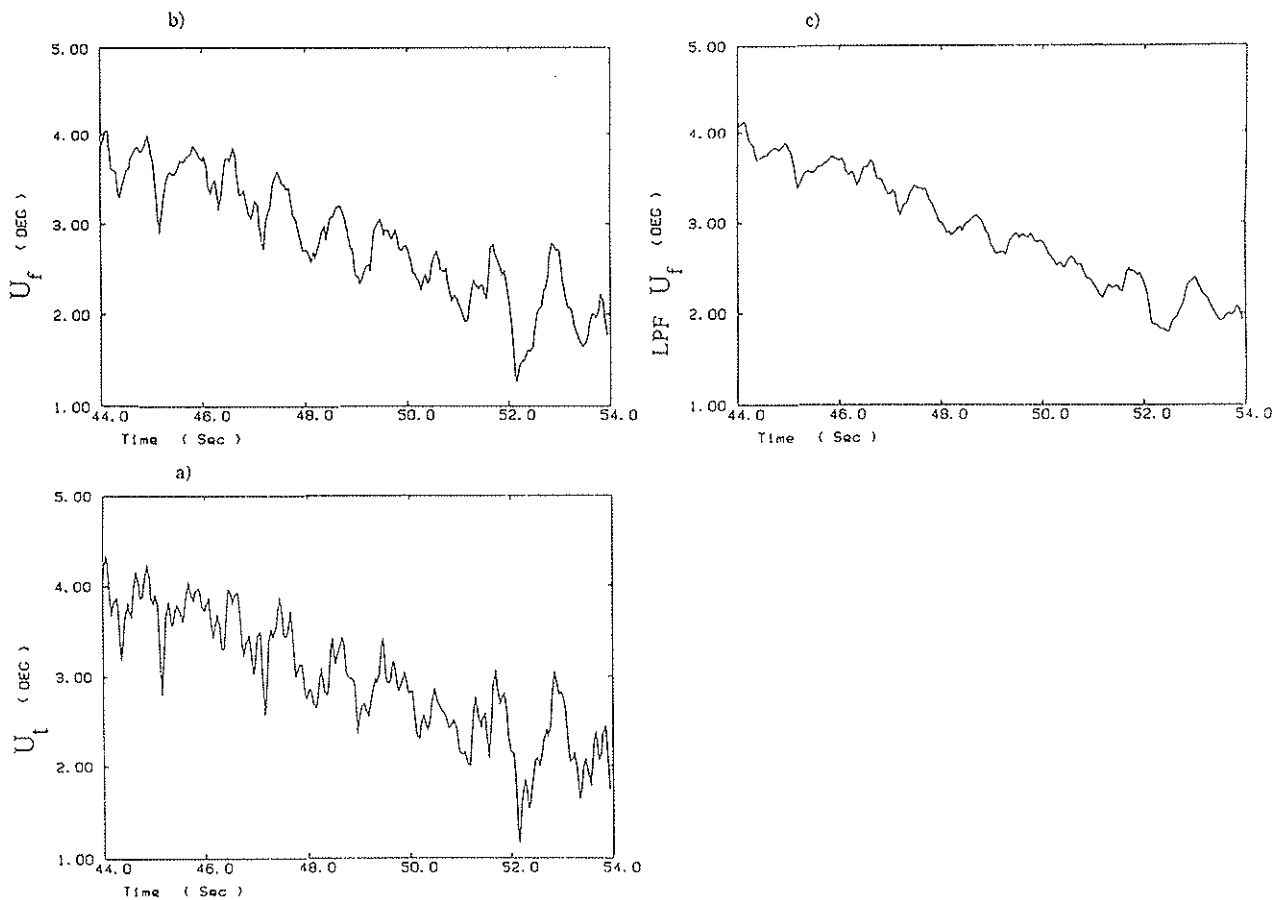

Fig 6. Sample time history of a) total head motion, U_t; b) estimated voluntary head motion, U_f; and c) low-pass filtered U_f during tracking of a continuously moving target.

Table 2. Average Results of Target Acquisition Experiment 2.

Configuration	Number of targets attempted	Percentage of targets captured (%)	Time per capture (sec)
Stationary	9.06	98.5	4.99
No filters	6.12	21.2	7.82
AF	6.47	46.2	6.95
LPF	8.09	86.8	6.14
AF + LPF	8.35	94.0	5.92

Improvement relative to no filtering (%)			
Configuration	Number of targets	Percentage of targets captured	Time per capture
AF	5.7	118	11.1
LPF	32.2	309	21.5
AF + LPF	36.4	343	24.3

captured, 98%, were quite high without vibration. Task performance, with the introduction of sinusoidal-only vibration was very poor, with the average of targets displayed falling 30% and the number of targets captured falling to 21%. Addition of the AF only resulted in an increase in the targets displayed by 6%, and the number of targets captured by 118%, relative to No Filtering. The LPF-only configuration produced a further increase in targets displayed, 32%, and a large percentage improvement in targets captured, 309%. Addition of the LPF to the AF further improved the number of targets presented to 36% and the number captured to 343% compared with No Filtering.

In Experiment 2, the improvement in performance between LPF and AF+LPF was slightly higher than in Experiment 1. The sinusoidal component of the vibration was the same for both tasks. The filters were not required to cope with the large random vibrations but still had to deal with the N_{na} generated as the result of a very precise positioning task combined with a minimum time-on-target constraint for score. The improved ability of the AF+LPF to deal with the additive biodynamic interference compared to the LPF was evident. The AF+LPF yielded a 7% increase in the number of targets captured and a 4% decrease in the average capture time.

An additional source of remnant excitation in the target acquisition task may have resulted from explicitly returning an indication of success or failure to the subject during each target appearance. Unlike the tracking task which required the continuous diligence of the subject and returned no explicit indication of tracking quality, the acquisition task elicited an intense effort to "score" for several periods of up to 10 seconds interspersed with short

periods of comparative relaxation. The resultant cyclical variation in muscle tension, breathing pattern, and overall level of anticipation and anxiety could have had a significant effect on the level of remnant experienced.

Large head movements for target acqusition with LPF and AF+LPF required subjects to slow their head motion just prior to the reticle intercepting the target to allow the reticle, with its attendant lag, to "coast" onto, or very near to the target. In the latter case, the additional head movements required to complete target acquisition were small and easily acomplished, due to well-tailored low-pass filtering of the nonadditive noise. All subjects agreed the resulting stabilized reticle response could be improved with reduction of the lag, but indicated that they rapidly became comfortable with the demonstrated head-following dynamics. They accepted the lag in favor of the improved dwell time and tracking precision.

Secondary Task Effects

At the start of the training period, all subjects were instructed that the targeting tasks were primary, with the tunnel-tracking effort secondary. The tunnel was to be followed to the best of one's ability but not at the expense of target tracking or acquisition.

Reaction to the manual tunnel-tracking task was very consistent across subjects. In the initial stages of training, all subjects found the secondary control task to be quite challenging when combined with the targeting tasks. This was particularly true of the target acquisition task in Experiment 2, where the static target with fixed exposure time forced the subject to fixate on the target to optimize the probability of capture. By the completion of the

training period, however, all subjects were accomplishing the primary tasks while consistently flying within the tunnel, largely with peripheral vision. By the end of actual production runs, the subjects generally agreed that the tunnel task did not significantly affect their perceived performance in the primary head tracking task.

Conclusions

A moving base ground simulation experiment was conducted to assess the contribution of various filter schemes to head-pointing precision during target tracking and acquisiton tasks while accomplishing a secondary vehicle control task. Pilot subject performance was measured under conditions of vertical vibration comprising both sinusoidal and random components. The results of this experiment indicate that the contribution of the adaptive filter to the helmet sight stabilization, in the presence of a random component in whole-body vibration, was small due to the dominance of the nonadditive biodynamic interference. However, the adaptive filter succeeded in suppressing most of the additive biodynamic interference component. The nonadditive biodynamic interference component, which is the dominant biodynamic interference component in pointing and tracking tasks, was successfully filtered by the low-pass filter. In general, all the subjects reached similar levels of performance. The tracking and pointing accuracy with the adaptive plus low-pass filter configuration proved to be the best, and in the case of the target tracking task, the results closely approached the pointing precision achieved without vibration.

The results generally agree with the previous preliminary single-axis studies and confirm the validity of the filtering schemes in the presence of a background vehicular control task.

Acknowledgments

References

1. Levison, W. H, Baron, S. and Junker, A. M., Modeling the Effects of Environmental Factors on Human Control and Information Processing, Wright-Patterson Air Force Base, Ohio, AMRL-76-74, Aug. 1976.

2. Jex, H. R., Problems in Modeling Man Machine Control Behavior in Biodynamic Environments, Proc. 7th Annual Conf. on Manual Control, NASA SP-281, 1971.

3. Wells, M. J. and Griffin, M. J., Benefits of Helmet Mounted Display Image Stabilization Under Whole-Body Vibration. Aviation, Space and Environmental Medicine, Jan. 1984.

4. Lewis, C. H. and Griffin, M. J., Predicting the Effects of Vertical Vibration Frequency, Combination of Frequencies and Viewing Distance on the Reading of Numeric Displays. Journal of Sound and Vibration, 1980.

5. Wells, M. J. and Griffin, M. J., Performance with Helmet Mounted Sights, ISVR Technical Report 152, University of Southampton, Sept. 1987.

6. Wells, M. J. and Griffin, M. J., Tracking with the Head During Whole-Body Vibration, In: Training, Human Decision Making and Control, J. Patrick and K. D. Duncan (Eds.), Elsevier Science Publishers, B.V. (North-Holland), 1988.

7. Lifshitz, S. and Merhav, S. J., Adaptive Suppression of Biodynamic Interference in Helmet Mounted Displays and Head Teleoperation, accepted for publication by the AIAA J. of Guidance, Control, and Dynamics.

8. Nicholson, R. M., The Feasibility of a Helmet Mounted Sight as a Control Device. Human Factors 8(5), pp. 417-425, 1966.

9. Grossman, J. D., Flight Evaluation of Pilot Sighting Accuracy Using a Helmet Mounted Sight, Naval Weapons Center, China Lake, California, Report No. NWCTP 5638, 1974.

10. Lifshitz, S. and Merhav, S., Man in the Loop Study of Filtering for Airborne Head Tracking Tasks. Submitted to the AIAA Journal of Guidance, Control and Dynamics.

11. Grunwald, A. J., Robertson, J. B. and Hatfield, J. J.,Experimental Evaluation of a Perspective Tunnel Display for Three-Dimensional Helicopter Approaches, AIAA Journal of Guidance and Control, Vol. 4, No. 6, Nov.-Dec. 1981, pp. 623-631.

12. Grunwald, A. J., Tunnel Display for Four-Dimensional Fixed Wing Aircraft Approaches. AIAA Journal of Guidance, Control and Dynamics, Vol. 7, No. 3, May-June 1984, pp. 369-377.

13. Grunwald, A. J., Predictor Laws for Pictorial Flight Displays, AIAA Journal of Guidance, Control and Dynamics, Vol. 8, No. 5, Sept.-Oct. 1985, pp. 545-552.

14. Widrow, B. and McCool, J. M., A Comparison of Adaptive Algorithms Based on the Method of Steepest Descent and Random Search, IEEE Trans. on Antennas and Propagation, Vol. AP-24, No. 5, Sept. 1976.

15. Merhav, S. J., Adaptive Suppression of Biodynamic Interference in Helmet Mounted and Head Down Displays. AIAA Guidance, Navigation and Control Conference, Minneapolis, Minnesota, Aug. 1988.

16. Haykin, S., "Adaptive Filtering Theory," Book, Prentice-Hall Information Systems Science Series, 1986.

17. Velger, M., Grunwald, A. and Merhav, S., Suppression of Biodynamic Disturbances and Pilot-Induced Oscillations by Adaptive Filtering, AIAA J. of Guidance, Control and Dynamics, July-Aug. 1984, pp. 401-409.

18. Velger, M., Grunwald, A. and Merhav, S., Adaptive Filtering of Biodynamic Stick Feedthrough in Manipulation Tasks on Board Moving Platforms, AIAA J. of Guidance, Control and Dynamics, Vol. 11, No. 2, March-April 1988.